PHYSICS AND CHEMISTRY OF SOLID STATE
V. 26, No. 4 (2025) pp. 895-904
Section: Physics

DOI: 10.15330/pcss.26.4.895-904

Vasyl Stefanyk Carpathian National University

ФІЗИКА І ХІМІЯ ТВЕРДОГО ТІЛА
Т. 26, № 4 (2025) С. 895-904
Фізико-математичні науки

PACS:75.50.Gg

ISSN 1729-4428 (Print)
ISSN 2309-8589 (Online)

Y.Kolekar Ravikumar[1], S.B.Kapatkar[2], S.N.Mathad[2], Sh. Hegde[3]

Magnesium-Doped Cobalt-Zinc Ferrite: A Study on Enhanced Magnetic and Electrical Properties

[1]*Physics Department, M.M.Arts& Science College, Sirsi (Uttara Kannada), Karnataka, India, ravikumarkolekar@gmail.com*
[2]*Department Physics , K.L.E. Technological University, Vidyanagar, Hubballi, India*
[3]*Department of Studies In Physics, Mangalore University, Mangalore, India*

This research investigates the synthesis, characterization, and properties of magnesium-doped cobalt zinc ferrite (Mg-Co-Zn ferrite) composites prepared by solid state reaction. Thermal analysis through TGA/DTG revealed phase formation and thermal stability, with weight losses corresponding to water and chloride evaporation, and the formation of metal oxides confirmed at 850°C. FTIR spectra identified the spinel structure, highlighting the effects of Mg^{2+} ion doping on lattice vibrations and cationic redistribution. Magnetic properties measured at room temperature (VSM analysis), exhibiting that Mg doping enhanced saturation magnetization (M_s) and coercivity (H_c), with super-paramagnetic behavior observed at the nanoscale. The dielectric constant of Mg-doped Co-Zn ferrite systems varies with Mg content, frequency, and hopping conduction, with the highest value at x = 0.08, attributed to Fe^{3+} ion migration. The study exhibits ferrites may be suitable for sensors, memory devices & high-frequency applications.

Keywords: Magnesium-doped Cobalt Zinc ferrite (Mg-Co-Zn ferrite), Solid-state reaction, Thermogravimetry, Fourier Transform Infrared Spectra, Vibrating Sample Magnetometer, Two probe.

Received 28October2024; Accepted 11November2025.

Introduction

Flexible oxide-based microwave composites are attracting much interest because of their good physical properties and possible applications in nanotechnology and microwave devices [1]. Spinel ferrites, which contain iron oxide, are magnetic ceramics with an immense potential for numerous scientific and technological applications [2]. Ferrites in their two forms–hexaferrite, which is hard, and spinel ferrite, which is mild–are notable candidates for use as electromagnetic materials due to their high electrical resistivity, nanoscaled size, and selectable physical and substance structures due to their strong chemical and thermal stability, ferrites in spinel form provide multifunctional materials used in a variety of fields, including biomedicine, catalysis, magnetic recording, and detection. C [2,3].

Some of these materials were created to have negative electromagnetic parameters in the radio frequency range 6–8GHz, and they have been widely used in many applications such as energy harvesting, space application, filter design, antenna design, electromagnetic absorber, etc [3-4]. They also contain Mg, Zn, Fe, Ag, or Co particles that are randomly dispersed in porous ferrite host. Furthermore, because flexible composites have excellent qualities, are inexpensive to fabricate, and are simple to synthesise, they are in high demand in the microwave communication system [3-4].

Researchers have developed different types of ferrites, such as $MgFe_2O_4$, $CoFe_2O_4$, $ZnFe_2O_4$, $Mg_xZn_{(1-x)}Fe_2O_4$& various ternary ferrites to achieve required tuning behaviour [5-6]. Magnesium Zinc Ferrite (Mg-Zn-Fe_2O_4) ferrite composed of Mg–Zn metal with a characteristic spinel assembly combined with iron oxide (Fe_2O_3). Te universal formulary $A_xB_{(1-x)}Fe_2O_4$, where "A" and "B" both are divalent transition ions. Te $MgZnFe_2O_4$ is fundamentally a dual oxide arrangement (MgO–ZnO–Fe_2O_2) that has maybe applicable as absorbents, semiconductors, and catalysts [5-7].

Mg-Zn-Fe_2O_4 are greatly influenced by the processes

used in synthesis method like hydrothermal, solid-state reaction, sol-gel, Co-precipitation, microwave methods and various mechano-chemical methods [6-8].

Cobalt ferrite is an inverse spinal with coercivity, arbitrate saturation magnetization, fine mechanical hardness, and chemical stability and finds mainly magnetic storage [9] & remarkable stability. Co-Zn ferrites, a combination possess excellent soft magnetic properties famous for their high electrical resistivity and are widely used in high-frequency applications, such as inductors and transformers for power supplies. Their high resistivity helps minimize eddy current losses, making them suitable for high-frequency applications [9-13].

Our work is novel because it systematically explores the substitution of Mg in Co–Zn ferrite composites, a topic that previous studies have not investigated thoroughly as they primarily focused on individual Mg-, Co-, or Zn-ferrites. We show that the structural, magnetic, dielectric, and electrical properties of Co-Zn spinel matrix can be distinctly affected by careful tuning of the Mg content, going beyond mere reporting of general trends. Our research specifically emphasizes the cationic redistribution shown by FTIR, the atypical increase of saturation magnetization and coercivity at certain Mg concentrations, and the finding that the maximum dielectric constant occurs at x = 0.08, which is associated with Fe^{3+} ion migration [14-16]. In addition, the relationship between Mg substitution and resistivity/conductivity via hopping mechanism offers new perspectives on charge transport in these composites. The results taken together establish Mg–Co–Zn ferrite as a multifunctional system with adjustable properties, showing great promise for microwave, magnetic recording, and biomedical applications. This sets our work apart from earlier isolated studies [16-19]. The previous research revealed the structural and surface morphological investigations of the Mg doped Co-Zn ferrites synthesised by solid state reaction [9]. On the other hand, we provide here, as a part of an earlier continuation, the effects of various Mg^{2+} ion replacement amounts on the structure and magnetic properties of Mg-Co ferrite. In the present study, we have characterised and evaluated reports on Fourier Transformation of Infrared Spectra (FTIR), Vibrating Sample Magnetometer (VSM) Hysteresis, AC Electrical Conductivity (Impedance work), and DC Electrical Conductivity using a range of experimental approaches.

I. Methodology

The process of preparing ferrites as shown in fig. 1 involves adding stoichiometric amounts of $ZnCl_2$, $FeCl_3$, MgO, and CO_3O_4 to a mortar and acetone. The reaction mass is pre-heated to 250°C for two to three hours. The crushed powders are then sintered in either air or oxygen for 5 hours at temperature 850°C, sometimes repeated until the mixture achieves the necessary crystalline phase. The sintered powders are further crushed to produce fine particles, and pellets. The final product is distinguished by various procedures after sintering the sample. The methodology is given in our previous publication [9]. Table 1 and 2 shows the stoichiometry and quantity of chemicals used for the synthesis process.

Table 1.

Atomic /molecular mass of raw materials

Name of the compound/atom	Molecular/atomic mass (g/mol)
$ZnCl_2$	136.29
$FeCl_3$	162.21
MgO	40.30
CO_3O_4	240.80

II. Results and Discussion

2.1. Thermogravimetric Analysis

The produced compound's thermal breakdown, stability, and temperature of phase formation are studied using TGA/DTG. The TGA and DTG curves obtained from the compound are displayed in Fig. 2. Examining the annealing temperature required for ferrite production is made easier by the thermal behaviour of the compound under investigation. At a consistent heating rate of 10°C/min, data is gathered from room temperature to 850°C. The weight loss in the TGA curve is 20% at 110°C and 25% at 180°C due to the evaporation of hydrated

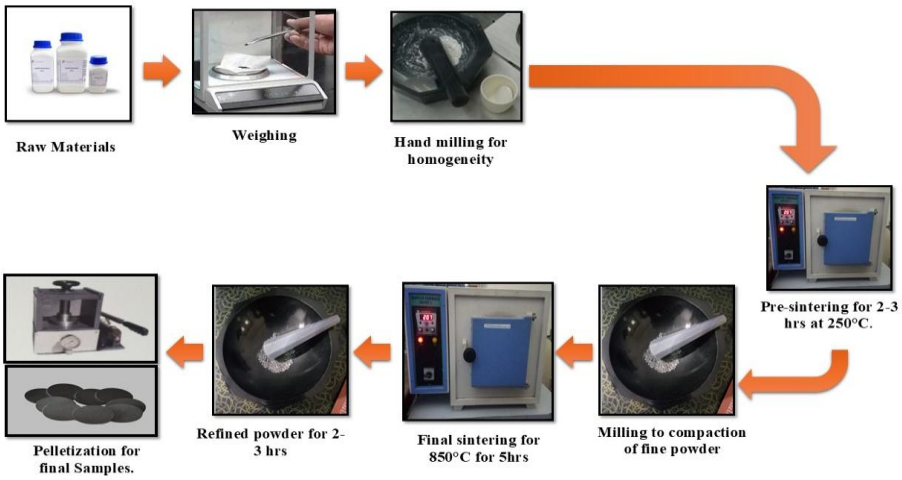

Fig. 1. Synthesis Method of Mg doped Co-Zn-Ferrite.

water, chlorides, and the conversion of hydroxide. DTG provides heat capacity, fusion, and material crystallisation are the causes of these weight losses [20]. DTG is helpful for identifying the temperatures or times at which specific decomposition steps occur, as these will appear as peaks in the DTG curve. In DTG curve there are two sharp peaks of endothermic at 90.37°C, 134.10°C (2 peaks of exothermic at ~110℃ and ~160℃).

The endotherm corresponds to absorption of external heat to decompose the material, while exothermic represents crystallization of the compound. The derivative loses between 90 ^{0}C to 134 ℃ are -3.382 %/min, -1.334 %/min. The broad Endotherm between 200℃ to 800℃ corresponds to absorption of external heat to decompose the material. Thus TGA/DTG confirms the formation of material or compound at 800 ºC to metal oxides [21].

2.2 Fourier Transform Infrared Spectroscopy

With tetrahedral and octahedral sites in the range of 400cm^{-1} to 4000cm^{-1}, the Mg doped Co-Zn ferrite's FTIR spectra provide information about its spinal structure and vibrations (Figure 3). The stretching vibration of the sample's -OH (H_2O bending mode) molecules is represented by the broadband absorption at 3433cm^{-1}. The weak absorption band present in the 1640 cm^{-1} shows the bending vibration of the -OH molecules. For x = 0.08 and 0.16, the cobalt ferrite system's distinctive absorption band at 1113 cm^{-1} may be the result of persistent FeOOH [22]. Two main vibrational modes, υ_1 and υ_2, with frequencies at 597 cm^{-1} and 403 cm^{-1}, respectively, are visible in the spectra. Stretching occurs at the interstitial tetrahedral [A] and octahedral [B] sublattices, respectively, at these two vibrational mode frequencies (υ_1 and υ_2). The different values of υ_1 and $\upsilon_2$show that the addition of Mg^{2+} ions to the zinc ferrite spinel matrix causes cationic redistribution. The variation and shifting of υ_1 and $\upsilon_2$values in zinc ferrite with an increase in Mg^{2+} substitution was reported by S.B. Somvanshi et al. The paper also reveals that, after the incorporation into regularly organized spinel zinc ferrite, Mg^{2+} ions accommodate at both interstitial sub-lattice spaces (A and B). Therefore, in the context of the current results, shifting of the (υ_1 and υ_2) values indicates that both interstitial sub-lattice positions (A and B) accommodate Mg^{2+} ions [23-25].

Fourier transform infrared (FTIR) spectra has been identify chemical residues, associated molecular bands, and the presence of functional groups in ferrite samples during the production process. The oscillation of the chemical link between the ions in the lattice is often responsible for the FT-IR absorption band observed in the produced ferrite samples. The FT-IR spectrum of ferrites in particular shows the presence of two primary wide metal oxygen energy bands in all spinels. Two primary absorption bands, spanning from 400 to 600 cm^{-1}, are visible in the FT-IR spectra. When Zn^{2+} ions are substituted into Mg-Co ferrite, the first absorption band is located about 400 cm^{-1}, while the second is located around 580 cm^{-1}. The absorption bands (υ_1 and υ_2) in the spinel structure are associated with the intrinsic lattice vibrations of octahedral and tetrahedral coordination, respectively. The stretching vibration of $M_{octahedral}$ O in octahedral position and the stretching vibration of the chemical bonds between tetrahedral position are responsible for the absorption band (υ_2) of 380-400 cm^{-1}. M $_{tetrahedral}\leftrightarrow$O shows an absorption band (υ_1) of 500-600 cm^{-1}. There is no characteristic peak υ_2 and because it is beyond the measuring range machine [25 REVIEW ALSO]. Spinel ferrite development was indicated by the observed

Table 2.

Calculation for 40 g Mg doped Co-Zn sample preparation

Composition	Need of CO_3O_4 (g)	Need of MgO (g)	Need of $ZnCl_2$ (g)	Need of $FeCl_3$ (g)
$Co_{0.8-x}\ Zn_{0.2}\ Fe_2\ O_4$	20.0468	----------	2.8706	17.083
$Co_{0.8-x}Mg_{0.08}Zn_{0.2}\ Fe_2\ O_4$	18.8251	0.3542	2.9953	17.825
$Co_{0.8-x}Mg_{0.16}\ Zn_{0.2}\ Fe_2\ O_4$	17.6139	0.7368	3.1149	18.5328
$Co_{0.8-x}Mg_{0.24}\ Zn_{0.2}\ Fe_2\ O_4$	16.0347	1.1640	3.2803	19.5209
$Co_{0.8-x}Mg_{0.32}\ Zn_{0.2}\ Fe_2\ O_4$	14.430	1.6294	3.4441	20.4959
$Co_{0.8-x}\ Mg_{0.40}Zn_{0.2}\ Fe_2\ O_4$	12.6575	2.1439	3.6252	21.5733
$Co_{0.8-x}\ Mg_{0.48}Zn_{0.2}\ Fe_2\ O_4$	10.6878	2.7154	3.8263	22.7703
$Co_{0.8-x}\ Mg_{0.56}Zn_{0.2}\ Fe_2\ O_4$	8.4867	3.3541	4.0511	24.1079

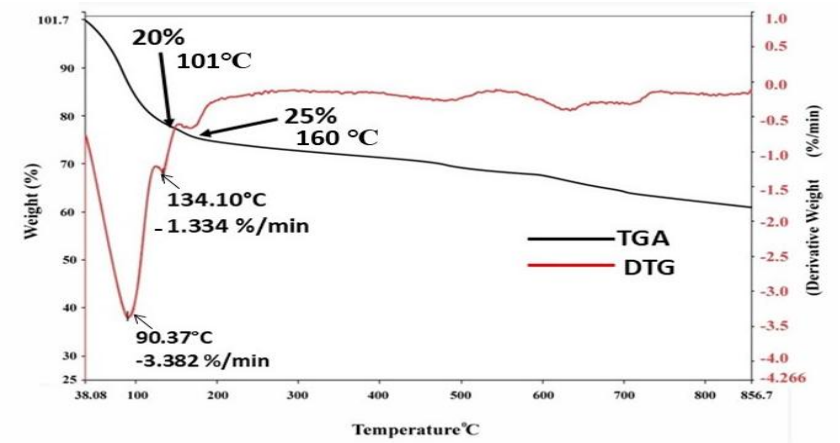

Fig. 2. TGA/DTG curvesfor $Co_{0.8-x}Mg_xZn_{0.2}Fe_2O_4$ferritewith x = 0.08.

significant peaks (υ_1). Free (or absorbed) water was thought to be present in the bands seen at 3420 and 1630 cm^{-1} that were linked to H-O-H stretching and bending patterns. The vibration of the remaining C-O bonds may be the cause of the peak at 1120 cm^{-1}. Stretching vibrations between C and H are what generate the absorption band at 1460 cm^{-1}. The peak near 1380 cm^{-1} might have been caused by the antisymmetric ferrite tetrahedral complexes' stretching vibrations. The ferrite lattice's bonding force, cation mass, and cation oxygen distance are all related to the chemical bond's vibration frequency. Additionally, it was noted that the absorption band's strength clearly dropped, particularly at x= 0.56 and 0.48 where the substitution concentration of Mg^{2+} ions was present. The fact that Mg^{2+} ions are added to the spinel structure explains this outcome. This is because divalent Mg^{2+} ions have a significant propensity to occupy spinel ferrite's tetrahedral configuration. Consequently, some Fe^{3+} ions in the original tetrahedron location will be replaced by more Mg^{2+} ions as the tetrahedron concentration increases, forcing them to migrate to the octahedron position and altering and impacting the absorption efficiency [26].

2.3 Vibrating Sample Magnetization

Hysteresis loops illustrate how the saturation magnetization (M_s) of artificially generated nanocrystalline materials varies with the applied magnetic field (H). Synthesized magnesium content cobalt zinc ferrites magnetic properties were characterized by VSM with an applied field of 15K Oe at room temperature. The M-H loops are used to study magnetic characteristics [Fig. 4]. Table 3 shows the obtained values for saturation magnetization, coercivity and retentivity. Saturation magnetization (M_s) increased from 3.52 to 55.7 emu/g, as well as coercivity (H_c) 183 to 324 Oe, except for x = 0.48. The cation distribution, where Mg^{+2}ions can transalate some of the Fe^{+3} to Fe^{+2} in B sites, is what causes the drop in M_s. In this case, the effective magnetic moment and Mg^{+2} ion radii are both to blame for the Ms decline. Decline of coercivity at x = 0.48, may be the presence of a significant amount of magnesium near grain boundaries results in a decrease in coercivity and makes domain wall movement more difficult. The range of retentivity is 1.12 emu/g to 14.02 emu/g, and it rises with Mg doping. An overabundance of Mg in the B site is shown by an increase in the magneto crystalline anisotropy K with increasing Mg doping [27, 28].

This hysteresis plot clearly demonstrates the influence of Mg substitution on the magnetic behavior of Co–Zn ferrites. The sample with x = 0.08 exhibits the highest saturation magnetization (~55.7 emu/g), confirming that moderate Mg^{2+} doping strengthens A–B superexchange interactions due to redistribution of Fe^{3+} ions into octahedral sites [29-30]. As Mg content increases beyond this point, Ms gradually decreases, with a sharp decline at x = 0.48, which indicates that excess non-magnetic Mg^{2+} dilutes the magnetic sublattice and promotes spin canting near grain boundaries. Coercivity also follows a similar non-linear trend, initially increasing with Mg substitution due to enhanced anisotropy but dropping at higher concentrations where grain boundary pinning weakens domain wall movement. The nearly S-shaped loops and narrowing at high Mg doping suggest the onset of

Table 3.

VSM data analysis of Mg doped Co-Zn Ferrites

Sl. No	x	Saturation Magnetization Ms (emu/g)	Coercivity Hc (Oe)	Retentivity Mr (emu/g)	Molecular. Wt (gm)	Magnetic moment $n_B(\mu_B)$	Remanance ratio Mr/Ms	Magnetic anisotropy K (erg/cm^3)
1	0.00	27.72	256	3.30	379.81	1.88	0.12	3548
2	0.08	55.7	324	14.02	366.745	3.63	0.25	9023
3	0.16	22.1	183	7.45	353.679	1.39	0.34	2024
4	0.24	29.6	255	8.73	340.612	1.77	0.30	3774
5	0.32	36.80	263	10.54	327.548	1.99	0.29	4839
6	0.40	38.36	272	10.97	314.48	2.17	0.29	5216
7	0.48	3.52	204	1.12	301.41	1.77	0.32	3539
8	0.56	39.45	310	13.3	288.35	1.90	0.34	6114

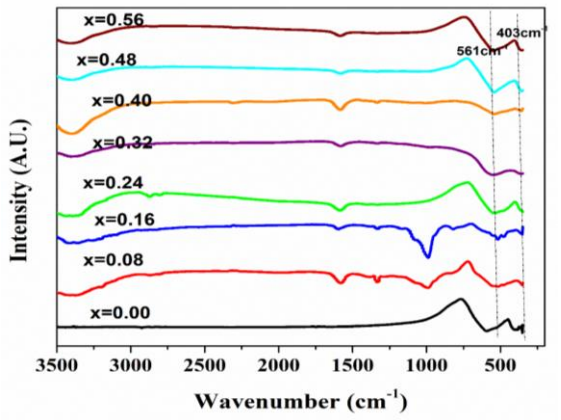

Fig.3. FTIR spectra of Mg-doped Co-Zn Ferrite.

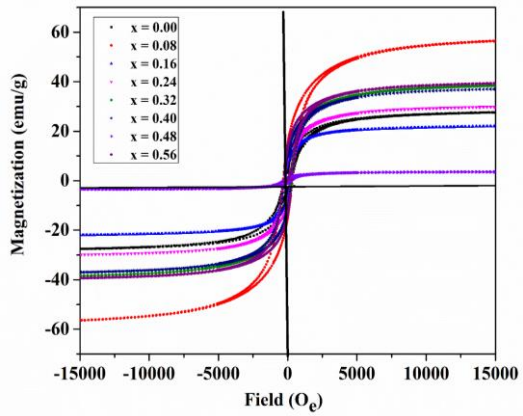

Fig. 4. Vibrating Sample Magnetometer Hysteresis loop of Mg doped Co-Zn Ferrite**.**

superparamagnetic-like features at the nanoscale. Overall, the figure highlights that controlled Mg doping provides a powerful way to tune magnetization, coercivity, and anisotropy in Co–Zn ferrite composites, optimizing them for specific high-frequency and memory device applications [29-31].

2.4. Dielectric studies through Impedance analyser (Ac)

Figure 5 illustrates the frequency response of the ferrite system's dielectric constant and plots the dielectric constant versus log frequency for each sample throughout a range of 40Hz to 5MHz. The graph indicates that at low A.C. fields, the dielectric constant rapidly decreases, approaches a minimum, and then stays constant at higher frequencies. The datas are depicted in tables 4 and 5. From the data, Dielectric constant for Mg-doped Co-Zn ranges from 11.58-18.75 and 4.38-8.81 for f = 0.5MHz and f = 4MHz. Dielectric loss at f = 0.5MHz and f = 4MHz for Mg doped Co-Zn lies between 2.44-11.17 and 0.32-3.51.A.C conductivity at f = 0.5MHz and f = 4MHz for Mg doped Co-Zn lies between $0.67 \cdot 10^{-6}$ – $3.09 \cdot 10^{-6}$S/cmand $1.27x10^{-6}$ - $7.82x10^{-6}$S/cm. Maximum dielectric constant of 18.75 at x = 0.08 for f = 0.5MHz which is more than undoped Co-Zn ferrite were observed. Dielectric constant decreases with Mg content except for x=0.24 possibly due to migration of Fe^{+3} ions from the octahedral site to the tetrahedral site. This decreases the hopping and hence decreases the polarization [32-34]. The Dielectric loss goes on increasing with respect to log f values. In low-frequency regions, the dielectric loss of Mg doped Cobalt Zinc Ferrite (particularly for x = 0.08) reaches very high. This is owing to the predominance of divalent Fe ions contributing to charge polarisation at grain boundaries [32-34]. From Koops' phenomeno-logical theory, dielectric dispersion means the dependence of the permittivity of a dielectric material on the frequency of applied electric field due to ever lagging relation between change in polarization and change in electric field, the permittivity of dielectric is a complex valued function of frequency (Hz). Hence Domain wall resonance loss factor curve is originated [32-36]. The dielectric constant drops as frequency increases because space charge transporters are unable to coordinate with the fast-changing electric field. The high dielectric constant at low frequencies is due to the resonance effect, which occurs when the frequency of charge transport between divalent and trivalent iron ions matches the applied field. The dielectric constant is influenced by oxidation conditions, synthesis procedure, and the limited solubility of Mg^{2+} ions, which might alter polarisation. The frequency-dependent change in AC conductivity at x = 0.08 Mg doped Cobalt Zinc Ferrite exhibits higher AC conductivity as frequency increases. The increase in AC conductivity is slower at low frequencies and faster at higher ones. This kind of electrical conduction mechanism is consistent with the electron hopping concept [35]. The rest of all composition samples had nonresponsive conductivity from log f 1 to 4. Then it is discovered to increase nearly exponentially up to a log f of 5 to 6 as the function frequency grows. The nonresponsive zone may reflect the direct current component of ac conductivity. The upward trend implies the AC component. The sudden rise in AC conductivity of Cobalt Zinc Ferrite with frequency is mostly due to enhanced hopping conduction, decreased resistance, effective dielectric relaxation, and improved charge carrier mobility at higher frequencies. These variables all contribute to the observed increase in AC conductivity [36-38]. The dielectric constant in Mg–Co–Zn ferrites varies due to factors such as cation distribution, charge carrier hopping, and grain boundary effects. At low frequencies, the high dielectric constant is attributed to space charge polarization caused by the build-up of charge carriers at grain boundaries, a process that is significantly affected by Fe^{2+}/Fe^{3+} hopping. The maximum dielectric constant observed at x = 0.08 indicates that moderate Mg^{2+} substitution promotes this hopping mechanism by driving Fe^{3+} ions into octahedral sites, thus increasing polarization. Nevertheless, when the Mg content increases beyond a certain point, the quantity of Fe^{2+}/Fe^{3+} pairs diminishes. This leads to a reduction in hopping probability and a subsequent decrease in the dielectric constant. Moreover, a greater substitution of Mg is associated with increased porosity and disruption of lattice symmetry, both of which contribute to the suppression of polarization. As the frequency increases, the dielectric carriers being unable to keep pace with the rapidly oscillating electric field, which means that only electronic constant stabilizes at lower values due to space charge and

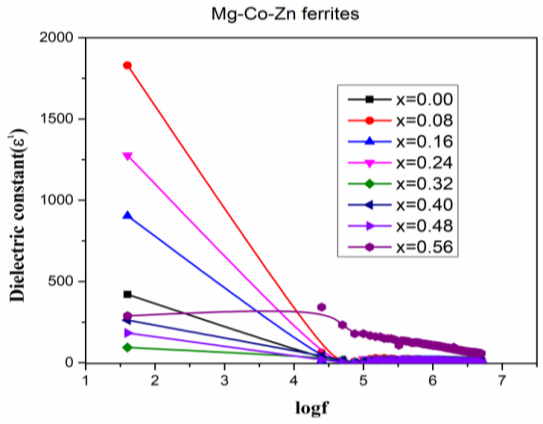

Fig. 5. FrequencyversusDielectricConstantofMgdopedCo-ZnFerrites.

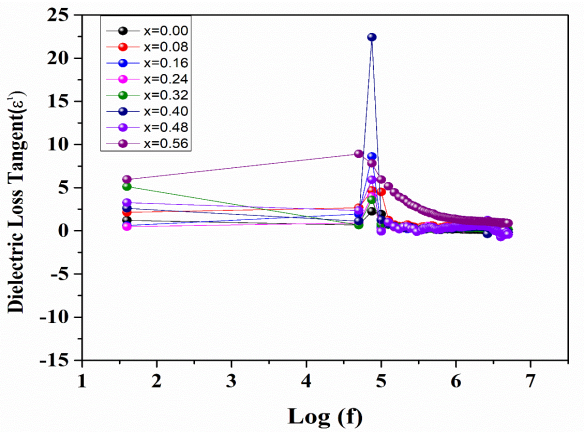

Fig. 6. Plot of Dielectric Loss tangent versus Log f of Mg doped Co-Zn ferrites.

Table 4.

Dielectric data at f = 0.5MHz for Mg doped samples

S. No.	x	Dielectric constant	Dielectric loss tangent	A C Conductivity (10^{-6} S/cm)
1	0.00	14.68	4.10	1.14
2	0.08	18.75	11.17	3.09
3	0.16	12.39	4.23	1.17
4	0.24	18.27	7.15	1.99
5	0.32	11.91	4.35	1.21
6	0.40	11.58	4.50	1.25
7	0.48	11.65	4.83	1.34
8	0.56	12.2	2.44	0.67

Table 5.

Dielectric data at f = 4.0MHz for Mg doped samples

S.No.	x	Dielectric constant	Dielectric loss tangent	A C Conductivity (10^{-6} S/cm)
1	0.00	14.68	4.10	1.14
2	0.08	6.04	3.51	7.82
3	0.16	7.78	2.03	4.53
4	0.24	7.61	1.57	4.37
5	0.32	8.81	1.44	3.20
6	0.40	5.17	0.85	1.89
7	0.48	4.38	0.32	7.08
8	0.56	6.04	0.57	1.27

ionic polarizations contribute. This tunable dielectric constant with Mg doping demonstrates the potential of Mg–Co–Zn ferrites in high-frequency applications where controlled dielectric behavior is required [39-42].

2.5. Electrical resistivity (DC)-Two probes

The behaviour of charge carriers can be understood through the study of electric properties, which is essential to comprehending the conduction mechanism in ferrites. For applications involving high frequencies, DC resistivity is essential. It depends on a number of variables, including density, porosity, particle size, and chemical makeup. The two-probe approach was utilized to ascertain the electrical resistivity of the pelletized sample that had been manufactured. From two probe method Resistance ($R = \frac{V}{I}$) and Resistivity ($\rho = \frac{RA}{l}$) at room temperature of the undoped Co-Zn ferrite, for Mg doped were calculated and tabulated in Table 6. Resistance and Resistivity of un doped Co-Zn are 396MΩ, 1038MΩ-cm Resistance of Mg doped Co-Zn lies between 93 MΩ to 902 MΩ. Resistivity lies between 183MΩ-cm to 3544MΩ-cm for Mg doped. So from the table 3.9 it is conclude that for Mg doped Co-Zn, resistivity is maximum (3544MΩ-cm) for x = 0.40 and it increases with Mg content [34-37]. Table 7 shows the Comparative Analysis of Structural, Dielectric, and Magnetic Properties of $CoFe_2O_4$-Based Ferrite Nanoparticles and Composites [28-29].

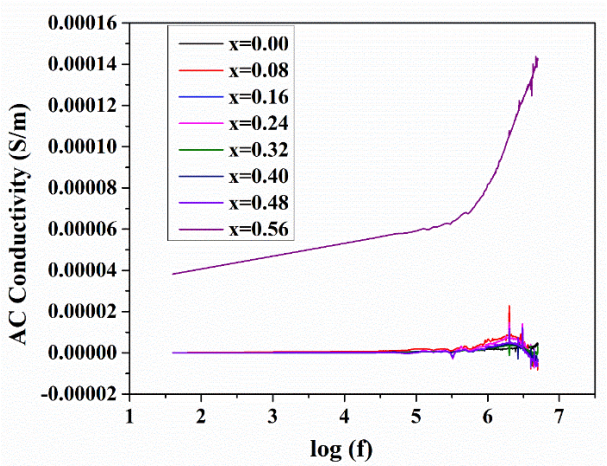

Fig. 7. AC conductivity versus log f of Mg doped Co-Zn ferrites.

Table 6.

D.C. Resistance and Resistivity at R-T of Mg doped samples

S. No.	x	Resistance (10^{+6} ohm)	Resistivity (10^{+6} ohm-cm)
1	0.00	396	1038
2	0.08	93	183
3	0.16	418	1096
4	0.24	605	2377
5	0.32	728	2860
6	0.40	902	3544
7	0.48	795	2498
8	0.56	311	698

Table 7.

Comparative Analysis of Structural, Dielectric, and Magnetic Properties of $CoFe_2O_4$-Based Ferrite Nanoparticles and Composites

Study	Method	XRD/SEM	FTIR	Dielectric	Magnetic (Hysteresis)	Re
Co0.5Zn0.5Cd 1.5xFe2-xO4 (Cd doped Co-Zn ferrites)	Coprepitaion (CPP), Solid state method (SSP)	cubic spinel structure, grain size less than1µm (CPP), granular, octahedral, tetrahedral shape having grain size in the range of 1-20 µm (SSR)	-	Dielectric constant (CPP: $4.54x10^2$–$1.1x10^6$, SSR: $2.7x10^3$-$3.9x10^5$ at 10Hz) increased with increase in Cd doping	-	[11]
Co0.5Ni0.5Cd 1.5xFe2-xO4 (Cd doped Co-Ni ferrites)	Coprepitaion (CPP), Solid state method (SSP)	XRD: cubic spinel structure, SEM: granular, agglomerated particles grain size less than 0.5 µm (CPP)	-	The dielectric constant decreases exponentially with respect to frequency.	-	[11]
Zn-$CoFe_2O_4$	Coprecipitation, 500°C	XRD: Cubic spinel	300–600 cm^{-1}	Not reported	Not reported	[44]
Mg-CoFe2O4	Gel method, annealed 700°C	XRD: Single-spinel Fd3m + α-Fe2O3, 15–17 nm	380 & 600 cm^{-1}	Specific capacitance 99.45 F/g	Ms & Mr ↓, Hc ↑ (low Mg) / ↓ (high Mg), FM→PM transition	[45]
Mg-Co-Zn	Citrate precursor	XRD: Single-phase spinel cubic Fd-3m, 37–47 nm	-	ε' 3.8–7.93, loss tangent 0.00095–0.081	Not reported	[46]
Co-Zn + CNT	Co-precipitation	XRD: Spinel cubic, crystallite size ↓ with CNT	Co-Zn ferrite & CNT peaks; shifts with CNT	Dielectric constant & loss ↑ with CNT	Saturation magnetization ↓ with CNT; Mmax = 34.351 emu/g	[43]
(Co0.6Ni0.4-xCdxFe2O4)	Co-precipitation	Cubic spinal, 14.52 and 16.92 nm (XRD), grain size- 0.85 to 0.21 µm(SEM).	400–600 cm^{-1}		Saturation magnetization: - 29.92 – 23.40 emu/gm & Coercivity:- 1113 to 708 Oe	[47]
Mg-Co-Zn Composite	Solid-state reaction	Spinel structure confirmed, phase at 850°C	Spinel lattice vibrations affected by Mg	Dielectric varies with Mg; highest at x=0.08; DC resistivity ↑ with Mg	Saturation magnetization (M_s) increased from 3.52 to 55.7 emu/g, coercivity (H_c) 183 to 324 Oe	*Present work

Conclusion

This study successfully synthesized and characterized Mg-Co-Zn ferrite composites, focusing on their structural, thermal, magnetic, and electrical properties. Thermal analysis via TGA/DTG indicated the formation of metal oxides and the phase stability of the compounds. FTIR spectra confirmed the spinel structure of Co-Zn ferrite. The study revealed significant changes in the magnetic properties, with Mg doping increasing saturation magnetization and coercivity. The composition with x = 0.08 displayed the greatest saturation magnetization (55.7 emu/g), increased coercivity (324 Oe), and peak dielectric constant (18.75 at 0.5 MHz), demonstrating a distinctive equilibrium between robust magnetic ordering and elevated polarization. These findings suggest that Co-Mg-Zn ferrite composites, with their tunable magnetic and electrical properties, are promising candidates for high-frequency applications, such as microwave absorption and magnetic recording. Additionally, their stability and superparamagnetic behavior make them suitable biomedical fields, sensors, and memory devices.

Acknowledgements:

Authors are thankful to Director and staff of STIC, Cochin University, Kerala for providing to charactering techniques such as TGA/DTG, XRD, SEM and FTIR for my experimental work. I would like to acknowledge IIT (CIF) Guwahati for VSM analysis. I also acknowledge Microtone, Mangalore University for providing Dielectric and Electric analysis as well as P.C.Jabin College Hubballi and KLEIT Hubballi for providing muffle furnace for sintering. Authors also would like to express my hat tip to the members of Modern Education Society, Sirsi for their motivation and support.

Conflict of interest:

All authors certify that they have no affiliations with or involvement in any organization or entity with any financial interest or non-financial interest in the subject matter or materials discussed in this manuscript.

***Kolekar Ravikumar Y.**– M.Sc, Ph.D, Associate Professor;*
***Kapatkar S.B.**– M.Sc, Ph.D, Professor;*
***Mathad S.N.**– M.Sc, Ph.D,Associate Professor;*
***Hegde Shreedatta** – M.Sc, Ph.D, Assistant Professor.*

[1] H. S.Mund, , and B. L. Ahuja, *Structural and magnetic properties of Mg doped cobalt ferrite nano particles prepared by sol-gel method*, Materials Research Bulletin, 85, 228 (2017); https://doi.org/10.1016/J.MATERRESBULL.2016.09.027.

[2] S.K. Sushant, N.J. Choudhari, S. Patil, *et al. Development of M–NiFe$_2$O$_4$ (Co, Mg, Cu, Zn, and Rare Earth Materials) and the Recent Major Applications*. Int. J Self-Propag. High-Temp. Synth. 32, 61 (2023); https://doi.org/10.3103/S1061386223020061.

[3] M. Abdullah Dar, et al. *Low dielectric loss of Mg doped Ni–Cu–Zn nano-ferrites for power applications*. Applied Surface Science, 258.14, 5342(2012); https://doi.org/10.1016/j.apsusc.2012.01.158.

[4] Y.Qu, H.Yang, N.Yang, Y.Fan, H. Zhu, and G.T.Zou, The effect of reaction temperature on the particle size, structure, and magnetic properties of coprecipitated $CoFe_2O_4$ nano particles. Materials Letters, 60(29–30), 3548 (2006); https://doi.org/10.1016/j.matlet.2006.03.055.

[5] H.Moradmard, et al. *Structural, magnetic and dielectric properties of magnesium doped nickel ferrite nanoparticles*. Journal of Alloys and Compounds, 650, 116 (2015); https://doi.org/10.1016/j.jallcom.2015.07.269.

[6] Kant, Ravi, and Ajay Kumar Mann. *A review of doped magnesium ferrite nanoparticles: introduction, synthesis techniques and applications*." IJSRSET 4.7 (2018).

[7] S. Kakati, M. K. Rendale, and S. N. Mathad, *Synthesis, Characterization, and Applicationsof CoFe2O4 and M-CoFe2O4 [M = Ni, Zn, Mg, Cd, Cu, Rare Earth materials (RE)] Ferrites (A review)*, Int. J Self-Propag. High-Temp. Synth., 30(4), 189 (2021);https://doi.org/10.3103/S1061386221040038.

[8] Nigam, Abhishek, and S. J. Pawar, *Structural, magnetic, and antimicrobial properties of zinc doped magnesium ferrite for drug delivery applications*. Ceramics International, 46(4), 4058 (2020); https://doi.org/10.1016/j.ceramint.2019.10.243.

[9] R.Y.Kolekar, et al. *Impact of Magnesium on Structural and Morphological Study of Co–Zn Ferrites*, International Journal of Self-Propagating High-Temperature Synthesis, 33(1), 58 (2024); https://doi.org/10.3103/s1061386224010047.

[10] K.V. Babu, B. Sailaja, K. Jalaiah, P.T. Shibeshi, M. Ravi, *Effect of Zinc Substitutionon the Structural, Electrical and Magnetic Properties of Nano-Structured $Ni_{0.5}Co_{0.5}Fe_2O_4$ Ferrites*, Phys. B, 534, 83 (2018); https://doi.org/10.1016/j.physb.2018.01.022.

[11] Kulkarni Akshay B, Mathad Shridhar N, Manohara S.R, Deshpande Sandeep M, Understanding, *Role of Cadmium Substitution on the Structural, Microstructural, Transport Properties of Ferrites Synthesized by Different Methods*, Science of Sintering, 56(4), 417 (2024);https://doi.org/10.2298/SOS240305010K.

[12] M.P. Reddy, A.M.A. Mohamed, X.B. Zhou, S. Du, Q. Huang, *A Facile HydrothermalSynthesis, Characterization and Magnetic Properties of Mesoporous $CoFe_2O_4$ Nanospheres*, J. Magn. MagnMater., 388 40 (2015); https://doi.org/10.1016/j.jmmm.2015.04.009.

[13] Rodríguez-Flores, Tatiana, Falak Shafiq, and Roberto Nisticò, *Synthesis, properties, and application in catalysis of Cu, Ni, Co, Zn ferrites: A comprehensive review study*. Journal of Alloys and Compounds, 1036, 181926 (2025); https://doi.org/10.1016/j.jallcom.2025.181926.

[14] Pendyala, Siva Kumar, et al. *Effect of Mg doping on physical properties of Zn ferrite nanoparticles.*Journal of the Australian Ceramic Society, 54,467 (2018);https://doi.org/10.1007/s41779-018-0173-8.

[15] A.B. Kulkarni, S.N. Mathad, *Variation in structural and mechanical properties of Cddoped Co-Zn ferrites*, Materials Science for Energy Technologies, 2(3),455 (2019); https://doi.org/10.1016/j.mset.2019.03.003.

[16] P.Saha, S.K. Shil, P.Roy, R.S. Auntu, N.I.Khan, &S.S. Sikder, *Exploring the structural, magnetic, dielectric and electrical properties of solid state method synthesized Mn3+ substituted Co–Zn ferrites*. Journal of Materials Science, 60(37), 17051 (2025); https://doi.org/10.1007/s10853-025-11449-6.

[17] Sharma Rohit, et al. *Improvement in magnetic behaviour of cobalt doped magnesium zinc nano-ferrites via co-precipitation route*, Journal of alloys and compounds, 684, 569 (2016); https://doi.org/10.1016/j.jallcom.2016.05.200.

[18] Eman E. El-Nahass, , et al. *Evaluation the toxic effects of Cobalt-Zinc Ferrite nanoparticles in experimental mice*. Scientific Reports, 15(1), 6903 (2025); https://doi.org/10.1038/s41598-025-90043-x.

[19] Numan Abbas, et al. *Investigation of structural, electrical and thermoelectric properties of cobalt-zinc ferrites/graphenenanocomposite*. Results in Physics, 59, 107576 (2024); https://doi.org/10.1016/j.rinp.2024.107576.

[20] S.M.Ansari, et al. *Effect of Manganese-Doping on the chemical and optical properties of cobalt ferrite nanoparticles*, Materials Science and Engineering: B, 300 117134 (2024); https://doi.org/10.1016/j.ssc.2021.114500.

[21] Verma, Kavita, Ashwini Kumar, and Dinesh Varshney, *Effect of Zn and Mg doping on structural, dielectric and magnetic properties of tetragonal CuFe2O4*, Current Applied Physics, 13(3), 467 (2013); https://doi.org/10.1016/j.cap.2012.09.015.

[22] Somvanshi, Sandeep B., et al. Influential diamagnetic magnesium (Mg2+) ion substitution in nano-spinel zinc ferrite (ZnFe2O4): thermal, structural, spectral, optical and physisorption analysis. Ceramics International, 46(7), 8640 (2020); https://doi.org/10.1016/j.ceramint.2019.12.097.

[23] Mukhtar Muhammad Waqas, et al. *Synthesis and properties of Pr-substituted MgZn ferrites for core materials and high frequency applications*. Journal of Magnetism and Magnetic Materials, 381, 173178 (2015); https://doi.org/10.1016/j.jallcom.2018.06.168.

[24] R.D. Waldron, *Infrared spectra of ferrites*, Physical review 99(6),1727(1955).

[25] A.S. Pujar, A.B. Kulkarni, S.N. Mathad, C.S.Hiremath,M.K. Rendale, M.R. Patil,R.B.Pujar, *Synthesis, Structural, FTIR and Electrical properties of* $Cu_xCo_{1-x}Fe_2O_4$ *(x= 0,0.4,1) Prepared by Solid State Method*, International Journal of self propagating high temperature synthesis, 27(3), 174 (2018);https://doi.org/10.3103/S1061386218030081.

[26] Saafan, Samia A., et al. *FTIR, DC, and AC electrical measurements of Mg Zn Nano-ferrites and their composites with Polybenzoxazine*. Applied Physics A, 127, 1 (2021); https://doi.org/10.1039/d3ra04557a.

[27] Patil, Kundan, *The effects of cobalt and magnesium co-doping on the structural and magnetic properties of* $ZnFe_2O_4$ *synthesized using a sonochemical process.*Solid State Communications 337, 114435 (2021); https://doi.org/10.1016/j.ssc.2021.114435.

[28] M. K. Shobana, *Photocatalytic and magnetic properties of Mg substituted cobalt ferrite*. Materials Science and Engineering: B 286, 116030 (2022); https://doi.org/10.1016/j.mseb.2022.116030.

[29] S.Kakati, S.Kuri, M.Rendale & S. Mathad,*Soft-Hard Ferrite Composites by Green Synthesis: Structural and Magnetic Properties.* Physics and Chemistry of Solid State, 26(2), 277 (2025); https://doi.org/10.15330/pcss.26.2.277-284.

[30] Hussain, Muneer, et al. T*uning the magnetic behavior of zinc ferrite via cobalt substitution: a structural analysis*.ACS omega, 9(2), 2536 (2024); https://doi.org/10.1021/acsomega.3c07251.

[31] B.Akshay Kulkarni, N. Shridhar Mathad, *Effect of cadmium doping on structural and magnetic studies of Co-Ni ferrites*, Science of Sintering, 53 (2021); https://doi.org/10.2298/SOS2103407K.

[32] Sarmah, Sikha, *A comparative study on the structural, magnetic and dielectric properties of magnesium substituted cobalt ferrites*, Ceramics International, 49(1), 1444 (2023); https://doi.org/10.1016/j.ceramint.2022.09.126.

[33] Chahar, Deepika, *Influence of Mg doping on the structural, electrical and dielectric properties of Co-Zn nanoferrites*, Journal of Magnetism and Magnetic Materials, 544, 168726 (2022); https://doi.org/10.1007/s10948-020-05565-4.

[34] Khan, Muhammad Zarrar, Iftikhar HussainGul, and Asad Malik. *Improved Electrical Properties Displayed by* Mg^{2+}*-Substituted Cobalt Ferrite Nano Particles, Prepared Via Co-precipitation Route*. Journal of Superconductivity and Novel Magnetism, 33, 3133 (2020); https://doi.org/10.1007/s10948-020-05565-4.

[35] Chahar, Deepika, *Influence of Mg doping on the structural, electrical and dielectric properties of Co-Zn nanoferrites*, Journal of Magnetism and Magnetic Materials, 544, 168726 (2022); https://doi.org/10.1016/j.jmmm.2021.168726.

[36] Pradhan, A. K., S. Saha, and T. K. Nath. *AC and DC electrical conductivity, dielectric and magnetic properties of* $Co_{0.65}Zn_{0.3}Fe_{2-x}Mo_xO_4$ *(x= 0.0, 0.1 and 0.2) ferrites*, Applied Physics A, 123,1 (2017);https://doi.org/10.1007/s00339-017-1329-z.

[37] M.A. Ahmed, *Electrical Properties of Co-Zn Ferrites*. Physica status solidi (a), 111(2), 567 (1989); https://doi.org/10.1002/pssa.2211110222.

[38] R. C. Bharamagoudar, J. Angadi V, A. S.Patil, L. B .Kankanawadi, S.N.Mathad, *Structural and dielectrical studies of nano Mn-Zn ferrites prepared by combustion method*,International Journal of Self-Propagating High-Temperature Synthesis, 28(2), 132 (2019); https://doi.org/10.3103/S1061386219020031.

[39] Ahmad, Syed Ismail, et al. *Dielectric, impedance, AC conductivity and low-temperature magnetic studies of Ce and Sm co-substituted nanocrystalline cobalt ferrite*. Journal of Magnetism and Magnetic Materials, 492 165666 (2019);https://doi.org/10.1016/j.jmmm.2019.165666.

[40] R.C. Bharamagoudar, A.S. Patil, S.N. Mathad, *Exploring the Influence of Zinc Doping on Nano Ferrites: A Review of Structural,* Dielectric, and Magnetic Studies. Int. J Self-Propag. High-Temp. Synth., 33, 165 (2024); https://doi.org/10.3103/S1061386224700110.

[41] M.U.Islam, et al. *Electrical transport properties of CoZn ferrite–*SiO_2 *composites prepared by co-precipitation technique*. Materials Chemistry and Physics, 109(2-3), 482 (2008); https://doi.org/10.1016/j.matchemphys.2007.12.021.

[42] Rakesh Vishwarup, Shridhar N. Mathad, Amir Altinawi, Raed H Althomali, Anish Khan, Ibraheem A Mkhalid, Khalid A Alzahrani, B C Anand, Vikas Gupta, *Effect of zinc substitution on structural, electrical, dielectric and magnetic properties of magnesium nano-ferrites prepared by co-precipitation route*, Inorganic Chemistry Communications, 167,112733 (2024); https://doi.org/10.1016/j.inoche.2024.112733.

[43] Ashok Kumar, *Structural, magnetic and dielectric properties of MWCNTs-incorporated Cobalt-Zinc Ferrite Nanocomposites*, Ceramics International, 51(16), 21470(2025); https://doi.org/10.1016/j.ceramint.2025.02.306.

[44] M.H. Jameel, et al. *Structural, optical and* morphological properties of zinc-doped cobalt-ferrites $CoFe_{2-x}Zn_xO_4$ (x=0.1-0.5), Digest Journal of Nanomaterials&Biostructures (DJNB) 16(2), (2021).

[45] Ali A. Ati, et al. *Structural, morphology, magnetic, and electrochemical characterization of pure and magnesium-substituted cobalt ferrite nanoparticles*, Journal of Materials Science: Materials in Electronics, 36(4), 252 (2025); https://doi.org/10.1007/s10854-025-14331-y.

[46] Chahar, Deepika, et al. *Influence of Mg doping on the structural, electrical and dielectric properties of Co-Zn nanoferrites*, Journal of Magnetism and Magnetic Materials 544, 168726 (2022); https://doi.org/10.1016/j.jmmm.2021.168726.

[47] P.Kashid, S. N. Mathad, & M. R. Shedam, *Impact of Cd^{+2} substitutions on structural and mechanical properties of $Co_{0.6}Ni_{0.4-x}Cd_xFe_2O_4$ ($0.00 \leq x \leq 0.40$) system*. Physics and Chemistry of Solid State, *24*(4), 595-602 (2023); DOI:10.15330/pcss.24.4.595-602.

Й. Колекар Равікумар[1], С.Б. Капаткар[2], С.Н. Матхад[2], Ш. Хегде[3]

Кобальт-цинковий ферит, легований магнієм: дослідження покращених магнітних та електричних властивостей

[1] Кафедра фізики, Коледж мистецтв і природничих наук М.М., м. Сірсі (Уттара-Каннада), штат Карнатака, Індія, ravikumarkolekar@gmail.com;
[2] Кафедра фізики, Технічний університет K.L.E., Віддьянагар, Хуббаллі, Індія;
[4] Кафедра фізики, Університет Мангалора, Мангалор, Індія

У роботі досліджено синтез, характеризацію та властивості композитів магній-легованого кобальт-цинкового фериту (Mg–Co–Zn ферит), отриманих методом твердофазної реакції. Термічний аналіз за допомогою TGA/DTG виявив стадії фазоутворення та термічну стабільність зразків, при цьому втрати маси відповідали випаровуванню води та хлоридів, а при температурі 850°Cпідтвердженоформування оксидів металів.ІЧ-спектри Фур'є (FTIR) ідентифікували шпінельну структуру та показали вплив легування іонами Mg^{2+} на коливання ґратки і перерозподіл катіонів. Магнітні властивості, виміряні при кімнатній температурі методом вібраційного магнітометра (VSM), засвідчили, що легування Mg підвищує намагніченість насичення (Ms) та коерцитивну силу (Hc), а в нанорозмірному стані спостерігається суперпарамагнітна поведінка.Діелектрична проникність систем Mg-легованого Co–Zn фериту залежить від вмісту Mg, частоти та механізмів стрибкоподібної провідності; максимальне значення зафіксовано при x = 0,08, що пов'язано з міграцією іонів Fe^{3+}. Отримані результати свідчать про перспективність таких феритів для застосування у сенсорах, запам'ятовуючих пристроях та високочастотних приладах.

Ключові слова: магній-легований кобальт-цинковий ферит (Mg–Co–Zn ферит), твердофазна реакція, термогравіметрія, інфрачервона спектроскопія Фур'є, вібраційний магнітометр, двозондовий метод.